Sensors and Materials, Vol. 36, No. 12 (2024) 5129–5141
MYU Tokyo

S & M 3857

MEMS Tactile Sensor for Mimicking the Response of Human Tactile Sensation

Ryusuke Mitobe,[1] Zhikai Geng,[1] Takashi Abe,[1]
Kensuke Kanda,[2] and Masayuki Sohgawa[1*]

[1]Graduate School of Science and Technology, Niigata University,
8050 Ikarashi 2-no-cho, Nishi-ku, Niigata 950-2181, Japan
[2]Graduate School of Engineering, University of Hyogo,
2167 Shosha, Himeji, Hyogo 671-2280, Japan

(Received July 16, 2024; accepted August 28, 2024)

Keywords: tactile sensor, MEMS, PZT, strain gauge, human tactile sensation

We report on the evaluation and measurement of a MEMS tactile sensor designed to mimic the temporal feature detection of human tactile sensation. The proposed sensor consists of a strain-resistive gauge and a piezoelectric thin-film capacitor on a microcantilever embedded in an elastomer. The cantilever is deflected by a force, which is detected simultaneously by the two separate sensing elements: the strain gauge and the piezoelectric thin film (piezoelectric sensor). The DC resistance change of the strain gauge is detected in time synchrony with the applied force. On the other hand, the piezoelectric sensor outputs a voltage owing to the formation of a polarized charge in response to the time variation of the applied force, and thus shows a time response different from that of the strain gauge. These could potentially reproduce the time-responsive nature of the human tactile function, which has receptive fields with different stimulus adaptation speeds. In this work, we demonstrated that different time response patterns can be obtained from each sensing element for the application of a single force or vibration.

1. Introduction

The current situation is that technologies for reproducing tactile sensations are not as widespread as those for visual and auditory sensations. In recent years, there has been much research on technologies to reproduce the sense of touch.[1–8] Haptics is needed in the fields of robotics and virtual reality, and is expected to develop further in the future.[9] Currently popular technologies for reproducing images and sounds require much arithmetic processing to reproduce realistic information at high resolutions, and thus require high-performance hardware. Unlike vision and hearing, the human sense of touch is a sensory organ that is not localized but distributed over the entire body surface[10], so the amount of information handled is large. Therefore, the number of sensor devices and the amount of information to be handled in the tactile reproduction technology are expected to become even more enormous. If a robot were to be equipped with a tactile perception mechanism like a human, the amount of wiring would be

*Corresponding author: e-mail: sohgawa@eng.niigata-u.ac.jp
https://doi.org/10.18494/SAM5241

ISSN 0914-4935
https://myukk.org/

so large that it would generate heat, which could lead to a breakdown in terms of implementability and information processing. To alleviate the problems of information volume collapse and energy consumption, it is necessary to devise ways to reduce the volume of tactile information handled in integrated processing. For this purpose, information processing at terminals (so-called "edge computing"[11]) is considered effective.

The tactile information that humans sense includes not only information such as the magnitude of force and temperature, but also temporal information such as their periodic change and change rate. The human skin is equipped with multiple tactile receptors with different temporal responses, which are classified into fast-adaptive (FA) and slow-adaptive (SA) receptors on the basis of their adaptation speed.[12] When humans recognize tactile information, they distinguish the temporal characteristics of the stimuli applied to the skin as a result of the differences in the adaptation and frequency sensitivity of these receptors.[13] These temporal characteristics of tactile information are necessary for the recognition of object texture and contact state. To handle such information, the data acquired by a tactile sensor requires preliminary processes, such as Fourier and wavelet analyses, which are often performed on software. We propose a tactile sensor in which the information input to the sensor is processed and output only by the sensor element by adjusting the output characteristics of the sensor similarly to a color filter in an image sensor. Figure 1 shows conventional tactile recognition and that to be achieved by the proposed sensor. By using such tactile sensors, it is possible to reduce the cost of subsequent information integration processing and realize an edge-processing–based model. In this study, we developed a MEMS tactile sensor that provides an electrical analog output with identified temporal features of tactile information, for the task of human tactile texture recognition.

We are working on the development of haptic sensors using MEMS technologies, which are easy to implement in devices.[14–24] In the sensor developed in this research, a DC strain resistor

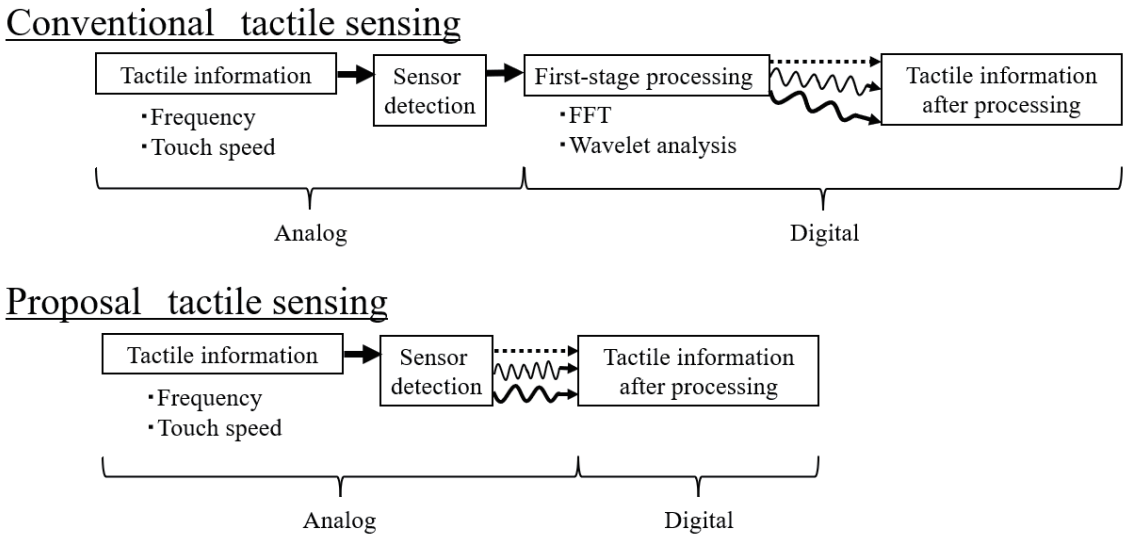

Fig. 1. Conventional and proposed tactile recognition tasks

(gauge) and a piezoelectric capacitor (piezoelectric sensor) are combined with a single microcantilever, which is the force detector of the MEMS tactile sensor developed in our previous works. These sensing elements have different time response characteristics to the applied tactile stimulus. This results in an analog output from the sensor in a form that reflects the temporal characteristics of the contact. In this paper, we describe how different temporal response patterns are obtained from each sensing element for a single applied force or vibration.

2. Materials and Methods

2.1 Sensor structure

Figure 2 shows (a) the overall view of the tactile sensor fabricated in this work, (b) a photograph of the sensor chip, and (c) an SEM image of the microcantilever. The sensor chip is 5.5 mm^2 and has microcantilevers on its surface that serve as the force detector. The microcantilevers are embedded in a polydimethylsiloxane (PDMS) elastomer. Figure 2(d) shows the cantilevers arranged in a circular pattern with three cantilevers at intervals of 120° to detect the direction of the shear load. We investigated the relationship between the size and shape of the cantilever and the sensitivity of the sensor, as well as the ability of the annular arrangement of

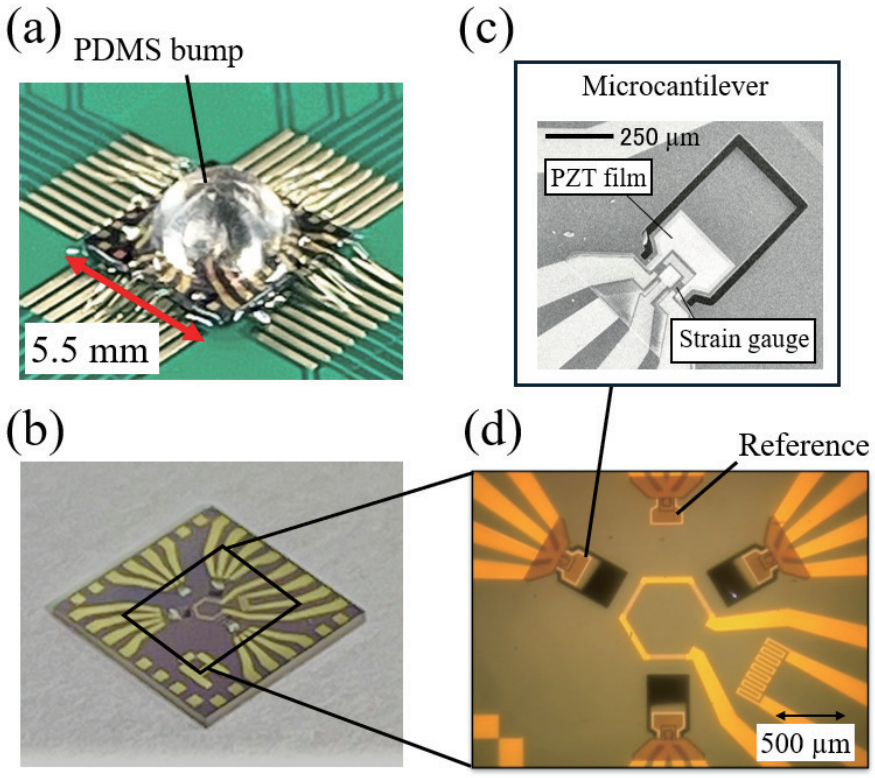

Fig. 2. (Color online) Photographs of (a) tactile sensor with PDMS bump mounted on PCB, (b) sensor chip with cantilevers, (c) SEM image of cantilever, and (d) cantilever arrangement on the chip.

the cantilevers to detect the direction of loading [14,24]. Figure 3 shows schematic diagrams of the top and cross-sectional views of the cantilever structure. The microcantilevers were fabricated on a Si-on-insulator (SOI) wafer using a bulk micromachining process. The sensing element on the cantilever consists of two parts: a wiring electrode and strain gauge made of Au and NiCr, and a capacitor structure consisting of a top electrode, piezoelectric part, and bottom electrode made of Pt, PZT, and Pt, respectively. A thermal dioxide (SiO_2) film was formed for the electrical insulation of the Si active layer forming the cantilever and the metal wiring. A polyimide film was also formed for the electrical insulation of the capacitor electrodes and strain gauges. The microcantilevers were spin-coated with PDMS and then covered with a hemispherical PDMS bump.

2.2 Detection principle

Figure 4 shows a schematic of the deformation behavior of the PDMS elastomer and cantilever when a normal force is applied to the sensor. The application of a normal force causes the PDMS elastomer to deform by sinking. This causes the cantilever to bend downward, leading to an increase in strain gauge resistance.

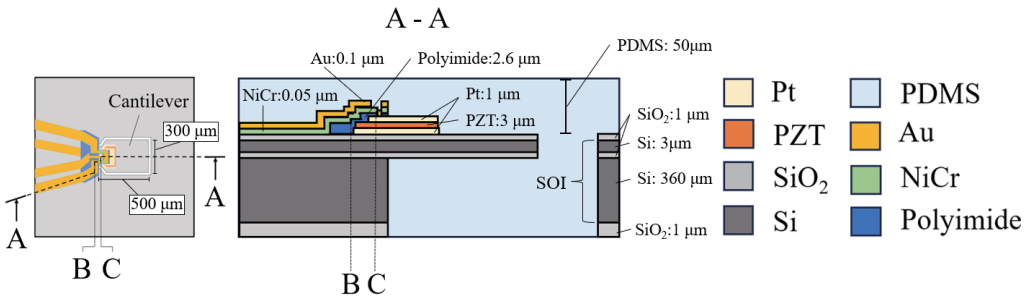

Fig. 3. (Color online) Schematic diagrams of the cantilever structure.

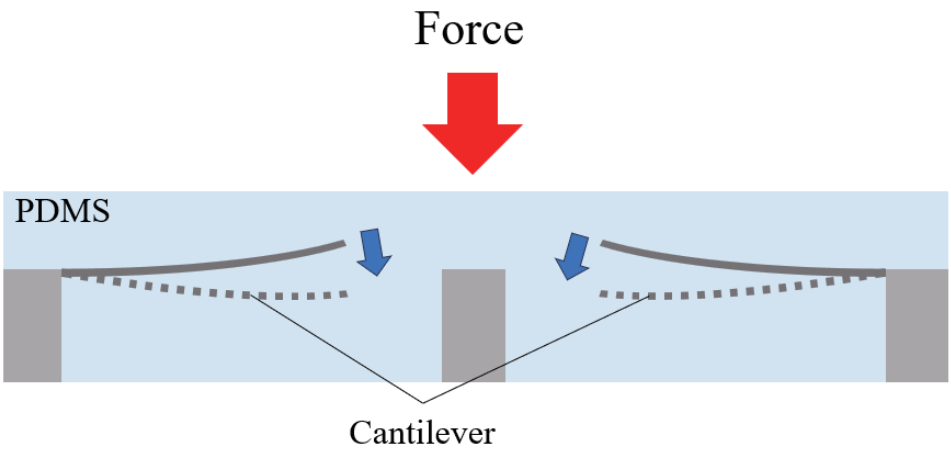

Fig. 4. (Color online) Schematic of the behavior of the elastomer and cantilever.

The change in surface strain caused by the deformation of the cantilever changes the electrical resistance of the strain gauge. From the change in the electrical resistance of the strain gauge, the external force applied to the sensor through the elastomer can be determined. The rate of change in the resistance $\Delta R/R$ of a strain gauge is given by

$$\frac{\Delta R}{R} = K_s \cdot \varepsilon, \tag{1}$$

where K_s is the gauge factor of the strain gauge material (NiCr) and ε is the strain. For example, if a strain gauge is subjected to tensile strain, the rate of resistance change, $\Delta R/R$, will also be positive because the strain ε is positive.

The change in strain associated with the deformation of the cantilever also deforms the piezoelectric material. When the piezoelectric material is deformed, a polarization charge is formed on the surface of the piezoelectric material as a result of the application of force, which in turn creates a polarization potential inside. This creates a voltage between the top and bottom electrodes of the piezoelectric material. The output charge density D of the piezoelectric sensor is given by the piezoelectric equation, using the piezoelectric constant d, the applied stress T, the electric field E, and the dielectric constant ε:

$$D = dT + \varepsilon E. \tag{2}$$

Since the current density I due to the voltage between the electrodes is the time-derivative component of the charge density, the voltage output that can be measured is the time-derivative component of the applied force.

$$I = \frac{dD}{dt} = e\frac{dT}{dt} + \varepsilon\frac{dE}{dt} \tag{3}$$

2.3 Sensor evaluation methods

A schematic of the experimental system used to measure the response to forces is shown in Fig. 5. In this experiment, a 3-axis motorized stage (Sigma Koki) was used to fix and move the sensor, and a 6-axis force sensor (SFS0036, Leptrino) was used to measure the applied normal force for reference. A digital multimeter (7481, ADC Corporation) was used to measure the electrical resistance of the strain gauge, and a digital lock-in amplifier (LI5650, NF Corporation) and an oscilloscope (RTM3000, Rohde & Schwarz) were used to measure the output of the piezoelectric sensor. This measurement system was used to measure the response of the sensor to the input mechanical deformation as the magnitude of the load and the thrust speed were varied. A 10-mm-diameter acrylic cylindrical indenter with a smooth surface that is sufficiently harder than the elastomer was used to apply the force. A schematic of the experimental system for measuring the sensor response to vibration is shown in Fig. 6. Vibration was applied by pushing in with an accelerometer attached to the vibration excitor (PET-0A, IMV). The output of

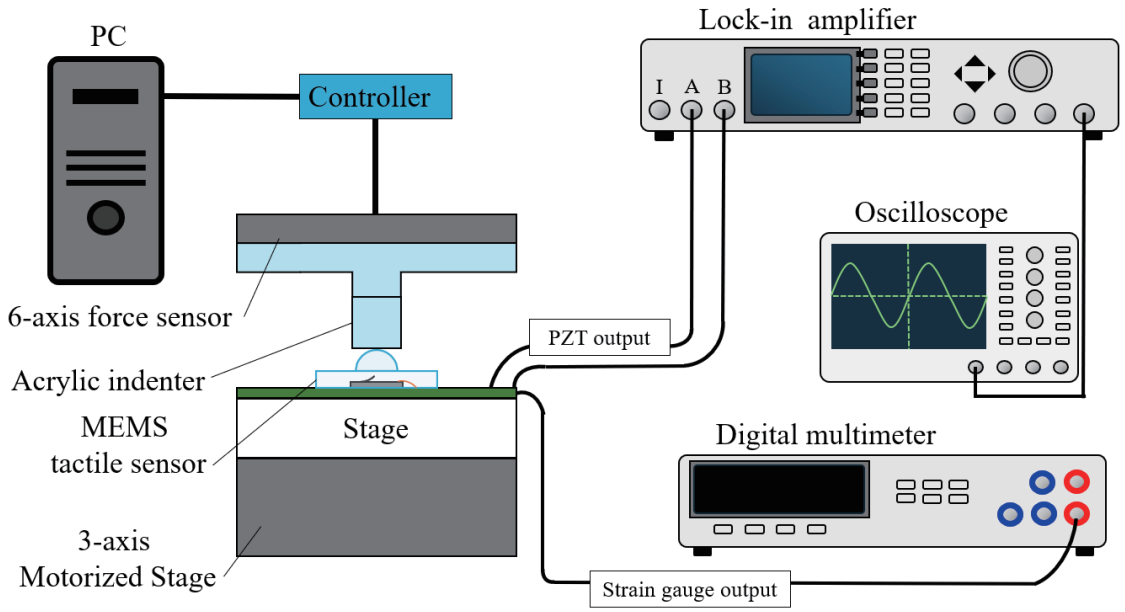

Fig. 5. (Color online) Schematic of the experimental setup for measuring the response to force.

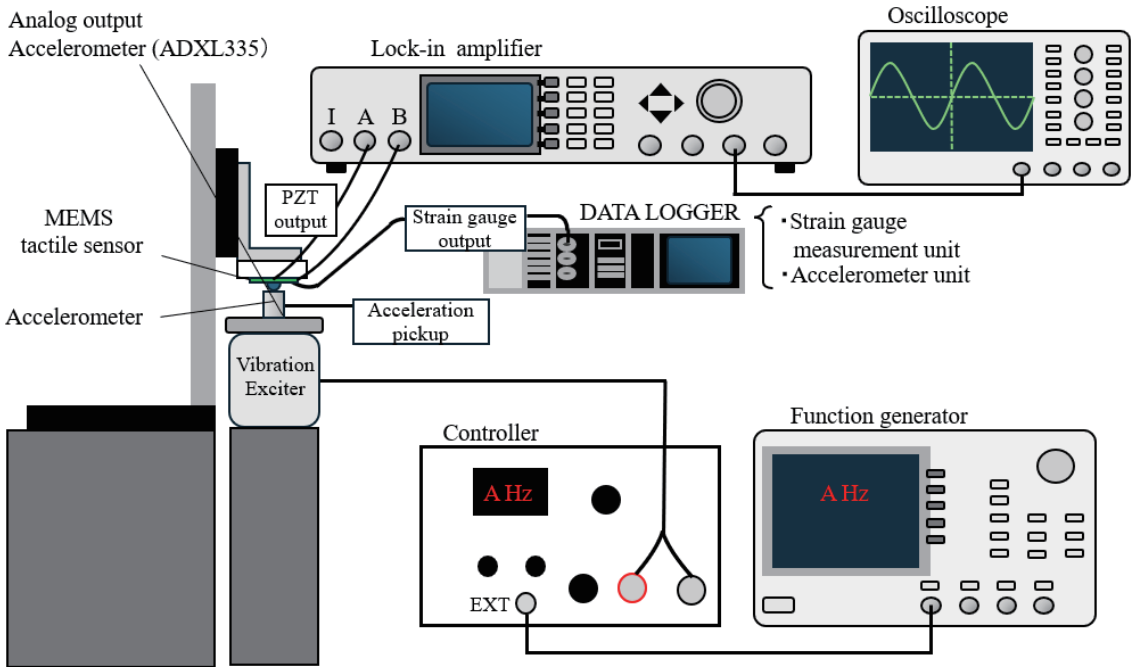

Fig. 6. (Color online) Schematic of the experimental setup for measuring the response to a vibration.

the strain gauge was measured using a Wheatstone bridge circuit inside the data logger (NR-600, Keyence), and the output voltage was measured using a strain gauge measurement unit (NR-ST04, Keyence). The output of the piezoelectric sensor was measured using a digital lock-in amplifier and an oscilloscope, as in the experimental system shown in Fig. 5. To confirm the

phase difference between the input and output with the sensor output, the displacement of the applied vibration was measured using an accelerometer (PV-85, Rion or ADXL 335, Analog Devices). The sensor was secured to the fixture by mounting it with screws using a fixture base made of polyoxymethylene (POM) resin with a sufficient hardness.

3. Results and Discussion

3.1 Transient response to normal force

Figure 7 shows the relationship between (a) the applied normal force and (b) the strain gauge resistance and (c) the output voltage of the piezoelectric sensor as functions of time, when a normal force of 1 N was applied to the sensor and then released. In this case, the speed of indenter movement was set to 5.0 mm/s and the force was held at 1 N for 2 s after application. When a force of 1 N was applied, the strain gauge exhibited a resistance change of approximately 3800 ppm from the initial resistance without applied force, and the resistance was maintained

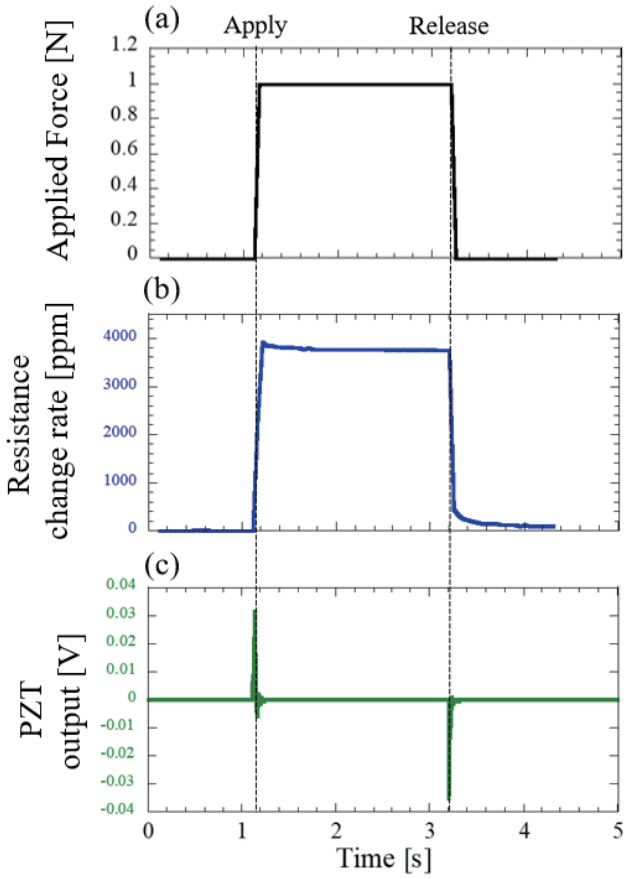

Fig. 7. (Color online) (a) Time history of the application of force. Outputs of (b) strain gauge and (c) piezoelectric sensor for applied force of 1 N shown in (a). The strain gauge continues to respond while force is applied and held without any change in the rate of change in resistance, whereas the piezoelectric sensor responds only at the time of the change in force during application and release.

while the applied force was held. In contrast, the piezoelectric sensor showed different positive and negative responses only when the force was applied and released, respectively, i.e., when the force changed over time. This characteristic response is due to the piezoelectric effect, where the charge output of the PZT capacitor corresponds to the time variation of the stress due to the applied force change. While the force does not change with time while the force is held, free electrons inside the PZT move to the side of opposite polarity to balance the potential between the electrodes, whereby the voltage between the electrodes decays and no output is generated. Thus, this sensor outputs an analog response from a single sensing element to an input of contact force in different patterns over time.

Figure 8 shows the (a) maximum (for applying) and (b) minimum (for releasing) outputs of the piezoelectric sensor at an indenter movement speed of 5.0 mm/s, as a function of applied force amplitude. According to Eq. (3), the quantity of charge is proportional to the output voltage amplitude. Hence, the sensor output voltage exhibits a linear relationship with the applied force amplitude in the range from 0.5 to 1.5 N.

Figure 9 shows (a) the rate of change in applied force and (b) piezoelectric sensor outputs at different indenter movement speeds with a constant applied force of 1 N. The indenter is pushed at speeds of 0.5, 1.0, and 5.0 mm/s from top to bottom in Fig. 9. From Eq. (3), the maximum output of the sensor is found to be larger when the speed is higher because the amount of change in applied force is greater. The output voltages integrated over time are 0.00026, 0.00027, and 0.00025 V•s for push-in speeds of 0.5, 1.0, 5.0 mm/s, respectively, which are approximately constant values independent of the speed of the applied force. This is because all applied forces are constant at 1 N, so the total charge is constant.

Figure 10 shows the sensor responses when external resistors with different resistances were connected in series with the piezoelectric sensor of the tactile sensor and normal force of 1 N was applied at a speed of 10 mm/s. Since the amplitude of the output voltage varies owing to the voltage drop across the external resistor, it is normalized to make easier to compare difference

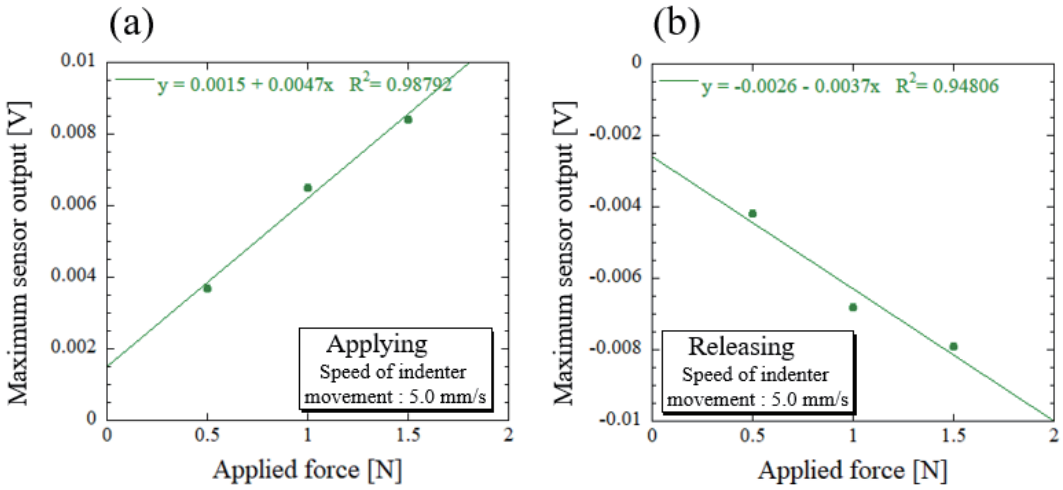

Fig. 8. (Color online) Dependence of the (a) maximum (for applying) and (b) minimum (for releasing) outputs of piezoelectric sensor on applied force amplitude.

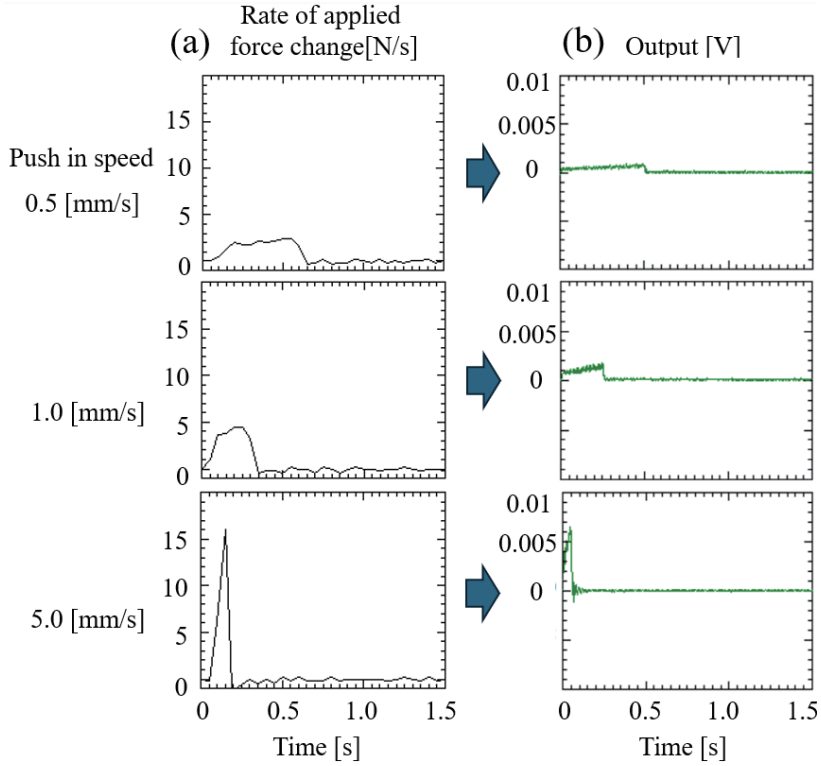

Fig. 9. (Color online) Relationship between (a) rate of change in applied force and (b) piezoelectric sensor output. Indenter speeds from top to bottom: 0.5, 1.0, and 5.0 mm/s.

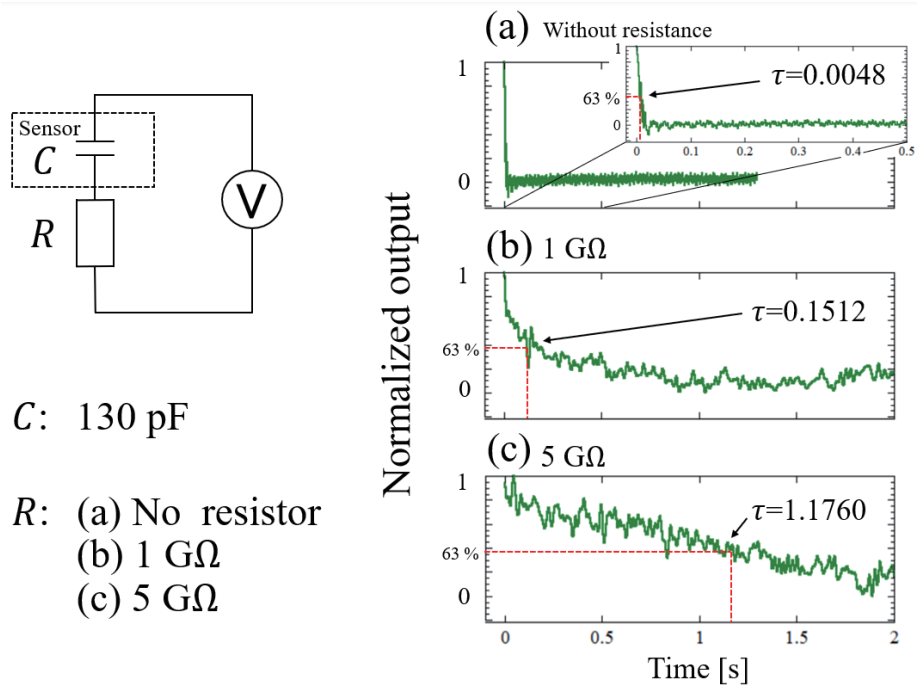

Fig. 10. (Color online) Time transient response and its time constant of the piezoelectric sensor (a) without an external resistor and with external series resistors of (b) 1 and (c) 5 GΩ. The output voltage is normalized to enable a comparison of time constants.

due to the time constant. The time constant τ of the discharge phenomenon of the charge accumulated on the electrodes of the capacitor is CR. τ is proportional to the series resistance and the capacitance of the piezoelectric sensor. As shown in Fig. 10(a), the time it takes for the output voltage in the transient state to decrease by 63% from the steady state is on the order of milliseconds. The time constant obtained from the decay of measured output is 0.0048 s. The capacitance of the piezoelectric sensor is 130 pF, which is estimated from the time constant τ to be about R = 37 MΩ. This is consistent with the nominal value of the input impedance of the measurement system and the order. Figures 10(b) and 10(c) show the measurement results when 1 and 5 GΩ resistors are connected, respectively. Although the larger value of the resistor caused an error due to the larger noise, the time constants obtained were 0.1512 and 1.1760 s, respectively, which are on the order of time compliant with the scale calculated from the resistor connected. As the resistance of the external resistor connected in series is increased, the time constant increases, indicating that the order of magnitude of the time constant can be adjusted by the circuit design of the sensor.

3.2 Frequency response

The response of the tactile sensor to the application of the periodic vibration was measured. Figure 11 shows the sensor outputs of each sensing element with the output of the reference accelerometer as the input vibration waveform (dashed line) and a 70 Hz vibration applied to the sensor. Figure 11(a) shows the sensor output voltage upon the resistance change of the strain gauge, measured using a bridge circuit. The output of the strain gauge is in phase with the periodic vibration applied to the sensor. On the other hand, as shown in Fig. 11(b), the output waveform of the piezoelectric sensor is shifted by about π/2 from the applied vibration. According to Eq. (3), the current density flowing is proportional to the time variation of the stress, and the resulting voltage is the time derivative of the stress. Therefore, the repeated application of cyclic forces such as vibration causes a phase advance in the output of the piezoelectric sensor.

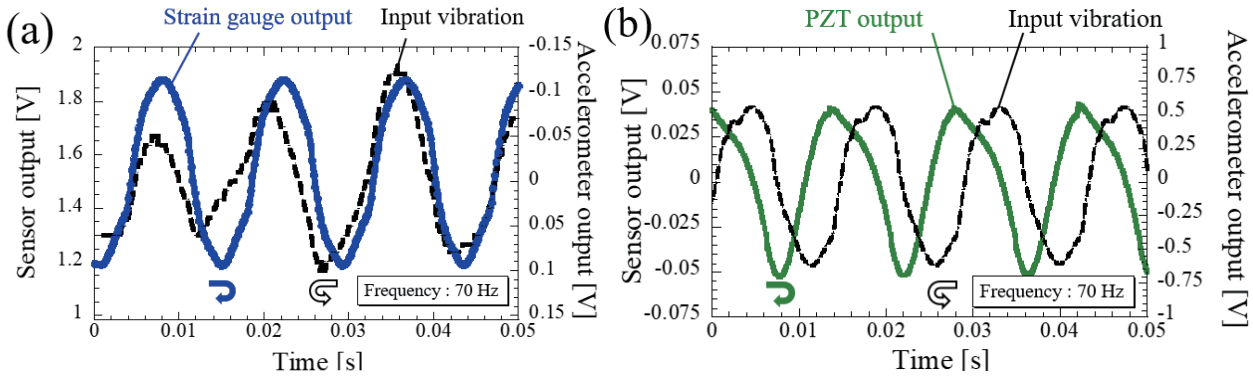

Fig. 11. (Color online) Sensor response to vibration. Outputs of (a) strain gauge and (b) piezoelectric sensor. The piezoelectric sensor has a phase advanced by 90°.

Thus, the sensor can generate different analog outputs with different phase characteristics from a single sensing element, even for inputs of vibration.

4. Conclusions

The research presented in this paper was focused on the development of a MEMS tactile sensor that is useful for edge computing. The innovative design of this sensor incorporates both a strain gauge and a piezoelectric sensor integrated on a single microcantilever structure to mimic the complex sensory mechanisms of human skin. The developed MEMS tactile sensor was shown to be able to provide different analog outputs for different temporal characteristics because of the dual sensing element and microcantilever design. For a normal force, the strain gauge resistor and the piezoelectric sensor were shown to provide different time-response outputs for different electrical properties. It was shown that the time response of the piezoelectric sensor can be controlled by an appropriate design of the electrical equivalent circuit. It was also shown that for periodic vibration, strain gauges produce a response output in phase with the applied input, whereas the piezoelectric output has a response that is 90° out of phase.

By inputting the analog output containing temporal features generated by sensors like the one we developed in this study, the processing cost of the touch recognition tasks using machine learning may be reduced. In turn, by making good use of the concept of predesigning sensor input/output characteristics in accordance with the task, as proposed in this study, it is expected that sensor development technology useful for edge processing will be developed.

Acknowledgments

This research is supported by JSPS KAKENHI-PROJECT JP22H01442.

References

1 K. Y. Tanaka: IEEJ J.Ind. Appl. **141** (2021) 80. (in Japanese).
2 R. S. Dahiya, G. Metta, M. Valle, and G. Sandini: IEEE Trans. Rob. **26** (2010) 1. https://doi.org/10.1109/TRO.2009.2033627
3 A. Takagi, Y. Yamamoto, M. Ohka, H. Yussof, and S. C. Abdullah: Procedia Comput. Sci. **76** (2015) 95. https://doi.org/10.1016/j.procs.2015.12.286
4 N. Thanh-Vinh, N. Binh-Khiem, H. Takahashi, K. Matsumoto, and I. Shimoyama: Sens. Actuators, A **215** (2014) 167. https://doi.org/10.1016/j.sna.2013.09.002
5 A. Spanu, L. Pinna, F. Viola, L. Seminara, M. Valle, A. Bonfiglio, and P. Cosseddu: Org. Electron. **36** (2016) 57. https://doi.org/10.1016/j.orgel.2016.05.034
6 G. Liang, Y. Wang, D. Mei, K. Xi, and Z. Chen: J. Microelectromech. Syst. **24** (2015) 1510. http://dx.doi.org/10.1109/JMEMS.2015.2418095
7 P. Goethals, H. Chaobal, D. Reynaerts, and D. Schaner: J. Clin. Monit. Comput. **28** (2014) 179. https://doi.org/10.1007/s10877-013-9513-y
8 M. H. Tippur and E. H. Adelson: Proc. 2023 IEEE Int. Conf. Soft Robotics. (2023) 1. https://doi.org/10.1109/RoboSoft55895.2023.10122097
9 T.-H. Yang, J. R. Kim, H. Jin, H. Gil, J.-H. Koo, H. J. Kim: Adv. Funct. Mater. **31** (2021) 1. https://doi.org/10.1002/adfm.202008831
10 J. Kanitakis: J. Eur. Acad. Dermatol. Venereol. **12** (2002) 390.
11 K. Iida: IEICE Tech. Rep. **117** (2017) 25. (in Japanese). http://hdl.handle.net/2115/86952
12 R. S. Johansson and Å. B. Vallbo: Trends Neurosci. **6** (1983) 27. https://doi.org/10.1016/0166-2236(83)90011-5

13 J. Dargahi and S. Najarian: Int. J. Med. Robot. Comput. Assist. Surg. **1** (2004) 23. https://doi.org/10.1002/rcs.3
14 H. Yokoyama, M. Sohgawa, T. Kanashima, M. Okuyama, T. Abe, H. Noma, and T. Azuma: Proc. SENSORS, 2013 IEEE. (2013) 1090. https://doi.org/10.1109/ICSENS.2013.6688401
15 H. Yokoyama, T. Kanashima, M. Okuyama, T. Abe, H. Noma, T. Azuma, and M. Sohgawa: IEEE Trans. Sens. Micromach. **134** (2014) 58. https://doi.org/10.1541/ieejsmas.134.58
16 M. Sohgawa, K. Watanabe, T Kanashima, M. Okuyama, T. Abe, H. Noma, and T. Azuma: Proc. SENSORS, 2014 IEEE. (2014) 1706. https://doi.org/10.1109/ICSENS.2014.6985351
17 M. Sohgawa, A. Nozawa, H. Yokoyama, T Kanashima, M. Okuyama, T. Abe, H. Noma, and T. Azuma: Proc. SENSORS, 2014 IEEE. (2014) 1749. https://doi.org/10.1109/ICSENS.2014.6985362
18 F. Sato, K. Takahashi, T. Abe, M. Okuyama, H. Noma, and M. Sohgawa: Sens. Mater. **29** (2017) 311. https://doi.org/10.18494/SAM.2017.1443
19 K. Takahashi, T. Abe, M. Okuyama, H. Noma, and M. Sohgawa: Sens. Mater. **30** (2018) 1091. https://doi.org/10.18494/SAM.2018.1786
20 R. Araki, T. Abe, H. Noma, and M. Sohgawa: Micromachines **9** (2018) 301. https://doi.org/10.3390/mi9060301
21 H. Takahashi, Y. Nanba, T. Abe, and M. Sohgawa: IEEJ Trans. Sens. Micromach. **139** (2019) 375. (in Japanese). https://doi.org/10.1541/ieejsmas.139.375
22 T. Fujihashi, F. Suga, R. Araki, J. Kido, T. Abe, and M. Sohgawa: J. Robot. Mechatron. **32** (2020) 297. https://doi.org/10.20965/jrm.2020.p0297
23 Y. Abe, T. Suga, T. Abe, H. Noma, and M. Sohgawa: IEEJ Trans. Sens. Micromach. **140** (2020) 272. (in Japanese). https://doi.org/10.1541/ieejsmas.140.272
24 R.Kaneta, T. Hasegawa, J. Kido, T. Abe, and M. Sohgawa: J. Robot. Mechatron. **34** (2022) 677. https://doi.org/10.20965/jrm.2022.p0677

About the Authors

Ryusuke Mitobe received his B.E. degree from Niigata University, Japan, in 2022 and his M.E. degree from the Graduate School of Science and Technology, Niigata University, Japan, in 2024. From 2024, he has been a doctoral student at the Graduate School of Science and Technology, Niigata University, Japan. He is currently engaged in research on tactile sensors. (ryusukemitobe@gmail.com)

Zhikai Geng received his B.E. degree from Shantou University, China, in 2021. From 2023, he has been a master's student at the Graduate School of Science and Technology, Niigata University, Japan. He is currently engaged in research on tactile sensors. (f23b146c@mail.cc.niigata-u.ac.jp)

Takashi Abe received his B.E. degree from Nagoya University, Japan, in 1992 and his M.E. and Ph.D. degrees from the Graduate School of Engineering, Nagoya University, Japan, in 1994 and 1997, respectively. From 2001 to 2003, he was an assistant at Tohoku University, Japan. From 2003 to 2010, he was an associate professor at Tohoku University, Japan. Since 2010, he has been a professor at Niigata University. His research interests are in quartz crystal MEMS, titanium microfabrication, and sensors. (memsabe@eng.niigata-u.ac.jp)

Kensuke Kanda received his Ph.D. degree from the Graduate School of Engineering, Tokyo Metropolitan University, Japan, in 2006. From 2010 to 2020, he was an assistant professor at University of Hyogo, Japan. Since 2020, he has been an associate professor at University of Hyogo, Japan. His research interests are in MEMS, actuators, quantum dots, particle tracking, piezoelectric thin films, PZT MEMS, and sensors. (kanda@eng.u-hyogo.ac.jp)

Masayuki Sohgawa received his B.E. degree from Osaka University, Japan, in 2000 and his M.E. and Ph.D. degrees from the Graduate School of Engineering Science, Osaka University, Japan, in 2002 and 2005, respectively. From 2007 to 2013, he was an assistant professor at Osaka University, Japan. From 2013 to 2016, he was an assistant professor at Niigata University, Japan. Since 2016, he has been an associate professor at Niigata University. He is currently engaged in research primarily focused on MEMS sensor devices such as tactile sensors and biosensors. (sohgawa@eng.niigata-u.ac.jp)